Hb/kg) or CO-HbV (1000 mg Hb/kg) at 30 min prior to the BLM treatment and 1 day after BLM treatment. Mice that were administered saline or HbV showed massive weight loss in response to the BLM treatment, whereas weight loss was suppressed in the case of CO-HbV administration (Figure 3A). Histopathological analysis (HE stain and Masson's trichrome stain) demonstrated that the BLM administration induced severe lung damage in the saline group (Figure 3B). In addition, the BLM treatment significantly increased the hydroxyproline content of the lung as compared with the control group (Figure 3C). These phenomena were all significantly suppressed by the CO-HbV treatment, but these effects were negligible in the case of the HbV treatment.

Moreover, to evaluate possible changes of respiratory function and lung mechanics associated with pulmonary fibrosis, we measured FVC and elastance. Based on data obtained using a computer-controlled ventilator, FVC clearly decreased in the BLM-treated mice and that this decrease was significantly suppressed by treatment with CO-HbV (Figure 3D). The changes in lung mechanics associated with pulmonary fibrosis are characterized by an increase in elastance. Total respiratory system elastance (elastance of the total lung, including the bronchi, bronchioles, and alveoli) and tissue elastance (elastance of the alveoli) increased following BLM treatment, effects that were partially restored by the administration of CO-HbV (Figure 3E and 3F). These results suggested that CO-HbV could be therapeutically beneficial for the treatment of BLM-induced pulmonary fibrosis.

Effect of CO-HbV on BALF cells, and inflammatory cytokines and chemokine levels in lung tissue

It is well-known that the inflammation plays an important role in the

pathogenesis of IPF, in view of the presence of interstitial and alveolar inflammatory cells as well as the expression of inflammatory cytokines in the lungs of patients with IPF [33, 34]. We postulated that the inhibition of pulmonary fibrosis by CO-HbV might contribute to the anti-inflammatory effect of CO [8, 9]. As an indicator of inflammation, the cells in BALF were analyzed. As a result, the administration of BLM resulted in a significant increase in the number of inflammatory cells (total cells: Figure 4A), alveolar macrophages (Figure 4B) and neutrophils (Figure 4C) on days 3 after BLM administration. The CO-HbV treatment significantly reduced all types of cells in the BALF.

We also examined the effect of CO-HbV on TNF-α, IL-6 and IL-1β levels in the lung tissue of BLM-induced pulmonary fibrosis at days 7. As shown in Figure 5, the levels of TNF-α (Figure 5A), IL-6 (Figure 5B) and IL-1β (Figure 5C) in lung tissue were increased by BLM were significantly decreased as the result of the CO-HbV treatment. These data suggest that CO-HbV exerts an anti-inflammatory action against BLM-induced pulmonary damage, and consequently ameliorates BLM-induced pulmonary fibrosis.

Effect of CO-HbV on ROS in lung tissue

A number of studies have suggested that the cellular redox state and the balance of oxidants/antioxidants play a significant role in the progression of pulmonary fibrosis in animal models and also possibly in human IPF [35]. To evaluate the effect of CO-HbV on ROS induced by the BLM treatment in the lung, immunostaining of 8-OH-dG and NO_2-Tyr, an oxidation product derived from nucleic acids and proteins, in lung sections were performed on day 3 after the BLM administration. As shown in Figure 6A, the

accumulation of 8-OH-dG (upper) and NO_2-Tyr (lower) in lung tissue increased in the BLM-treated mice as compared to control mice, while CO-HbV clearly suppressed the levels of these oxidative stress markers in the lungs.

Recent reports have suggested that ROS generation by the Nox family NADPH oxidases, especially Nox4, might be implicated in the pathogenesis of IPF [36, 37]. In order to evaluate the ROS derived from Nox4, we examined superoxide production in lung tissue. As a result, the BLM treatment showed an obvious increase in superoxide production, Nox4 activity, while CO-HbV treatment suppressed superoxide production (Figure 6B). However, no difference in the protein expression of Nox4 between saline and CO-HbV was found, as evidenced by immunostaining and western blotting analysis (Figure 6C and 6D). Although very little is known concerning the pathway of Nox4 activity, it is well known that $p22^{phox}$ and Poldip2 are important regulators of Nox4 activity [38]. Thus, we next determined the protein expression of $p22^{phox}$ and Poldip2 at 7 days after BLM administration. Similar to the increase in the protein expression of Nox4, the protein expression of $p22^{phox}$ was also increased by BLM treatment (Figure 6E). On the other hand, the protein expression of Poldip2 was decreased by the BLM treatment (Figure 6F). Interestingly, no change was found in the expression of both $p22^{phox}$ and Poldip2 between the saline and CO-HbV treatment (Figure 6E and 6F). These results indicate that CO derived CO-HbV suppressed the superoxide production generated by Nox4 without any detectable changes in the protein expression of Nox4, $p22^{phox}$ and Poldip2, indicating that CO suppressed Nox4 activity *via* a currently unknown pathway.

Effect of CO-HbV on active TGF-β1 levels in lung tissue

TGF-β1 has been reported to play pivotal roles in the progression of pulmonary fibrosis,including fibroblast proliferation and collagen deposition [39]. To reveal the mechanism underlying the suppressive effect of CO-HbV on BLM-induced pulmonary fibrosis, the levels of active TGF-β1 in lung tissue on day 14 were determined. As shown in Figure 7, the level of active TGF-β1 was increased in the BLM-treated mice, while CO-HbV decreased the level of active TGF-β1 to the same level as the control group.

Discussion

In present study, we evaluated the therapeutic effects of CO-HbV on IPF and investigated the impact of CO on the pathogenesis of IPF using a BLM-induced pulmonary fibrosis mice model. Three major findings were uncovered in the investigation. First, CO-HbV suppressed the progression of pulmonary fibril formation and improved respiratory function. Second, the mechanism underlying the suppressive effect of CO-HbV on BLM-induced pulmonary fibrosis can be attributed to the anti-oxidative and anti-inflammatory effects of CO. Furthermore, ROS generation was decreased as the result of the inhibition of the activity of the NADPH oxidase family, which is an important role in the pathogenesis of IPF, with no detectable changes in its protein expression. Finally, it can be concluded that HbV has considerable potential for effectively delivering CO to the lungs, suggesting that CO-HbV has promise for use as an effective CO donor.

Guidance on the diagnosis and management of IPF updated by the American Thoracic Society (ATS), European Respiratory Society (ERS), Japanese Respiratory Society (JRS) and Latin American Thoracic Association (ALAT) gave a 'weak no' recommendation to pirfenidon therapy, which is only drug approved for clinical use. Use of the drug can produce side effects (photosensitivity) and its effect on reducing pulmonary issues is small [40]. Therefore, it is important to examine the effect of candidate drugs on the progression of pulmonary fibrosis, lung mechanics as well as side effects. In the present study, severe pulmonary fibrosis induced by BLM was dramatically suppressed by intravenous CO-HbV administration (Figure 3B and 3C). Furthermore, CO-HbV suppressed a BLM-induced increase in lung elastance and a decrease in FVC (Figure 3D-F), indicating that CO-HbV could be beneficial for the treatment of patients

with IPF. In addition, there were no changes of serum laboratory parameters reflecting hepatic, renal and pancreatic function for the experimental period after CO-HbV administration, compared to saline treatment in BLM-induced pulmonary fibrosis mice (Table 1). However, cholesterol levels were significantly elevated at 7 days after the administration of CO-HbV. This is likely derived from metabolites contained by the HbV particles because they contain a large amount of cholesterol for structural stabilization and efficient Hb encapsulation. In a study using healthy mice and rats, we demonstrated that the added cholesterol was completely eliminated in the feces *via* biliary excretion within 14 days after the administration of HbV [41]. In fact, the serum cholesterol levels at 14 days after CO-HbV administration was not different compared to that in saline administration in this study. These results indicate that CO-HbV could suppress the progression of pulmonary fibrosis and the decline of lung mechanics without any severe side effects, thus, represents a promising candidate agent for novel IPF treatment.

Although the pathogenic mechanisms of IPF are unknown, a growing body of evidence suggests that both chronic inflammation and ROS (among other issues) appear to play a role in the onset or progression of IPF. Previous studies using human subjects with IPF have demonstrated that the generation of ROS from alveolar inflammatory cells, such as neutrophils and macrophages is enhanced and that this may promote alveolar epithelial cell injury and induce chronic inflammation, thus initiating or contributing to the development of pulmonary fibrosis [42, 43]. In the present study, CO-HbV suppressed the cells count in BALF including neutrophils and alveolar macrophages (Figure 4), and reduced the production of oxidation products (8-OH-dG and NO_2-Tyr), derived from nucleic acids and proteins, in the lung (Figure 6A). In addition, the levels of cytokines (TNF-α , IL-6 and IL-1β) in lung tissue were significantly decreased as the

result of the CO-HbV treatment (Figure 5). It is well-known that inflammatory cells, including neutrophils and alveolar macrophages, are able to produce ROS via Nox2, which are essential to the development of pulmonary fibrosis in BLM-induced IPF model mice [44]. Nakahira et al. reported that ROS production was inhibited in LPS-treated macrophages when the cells were exposed to CO [45]. In addition, they also concluded that that CO can form a complex with Nox2, indicating that CO is likely to modulate Nox2 activity [45]. These data suggest that CO-HbV would exert an inhibitory effect on the production of Nox2 in inflammatory cells, resulting in ameliorating the initiation and progression of BLM-induced pulmonary fibrosis.

In addition to Nox2, ROS are also generated by Nox4 and play a crucial role in the induction of alveolar epithelial cell death and the subsequent development of pulmonary fibrosis. In fact, it has been reported that Nox4 expression was increased in pulmonary fibrosis from patients with IPF [36, 37], and the genetic or pharmacologic targeting of Nox4 abrogated fibrogenesis in murine models of lung injuries [37, 46]. In our study, the Nox4 activity was suppressed by the administration of CO-HbV (Figure 6B). Previously, the activity of Nox4, as determined by ROS generation, was thought to be exclusively dependent on the protein levels of Nox4 *in vitro* [47]. Interestingly, contrary with a previous *in vitro* study [47], our *in vivo* data using BLM-induced IPF model mice showed that the protein expression of Nox4 remained unchanged after the saline, HbV and CO-HbV treatment in BLM-induced IPF model mice (Figure 6C and D). Although the activation mechanisms of Nox4 are largely unknown, at least part of the $p22^{phox}$ and Poldip2 would be related to Nox4 activity [38]. Therefore, we hypothesized that CO affected Nox4 activity via the membrane translocation of these two regulators, namely, $p22^{phox}$ and Poldip2. However, the protein expression of $p22^{phox}$ and Poldip2 in

plasma membranes were not changed among the saline, HbV and CO-HbV treatment in BLM-induced IPF model mice (Figure 6E and F). It therefore appears that CO inhibits a currently unknown pathway of Nox4 activation. A possible explanation for this issue is that CO interacts directly with the heme contained in Nox4. In fact, an interaction of Nox2, a heme protein, with CO was recently confirmed by a spectroscopic analysis [45]. Further investigation regarding this mechanism will be necessary to develop a comprehensive understanding of the effect of CO on tissue fibrosis.

There is an increasing body of evidence to suggest that epithelial-mesenchymal transition (EMT), a process whereby fully differentiated epithelial cells undergo a transition to a mesenchymal phenotype, thus giving rise to fibroblasts and myofibroblasts, may play a substantial role in a variety of pathogenic processes during pulmonary fibrogenesis. TGF-β1 has been implicated as functioning as a master switch in the induction of fibrosis in the lung, and is a major mediator of EMT in a number of physiological contexts, including pulmonary fibrosis [48]. In this regard, TGF-β1 is upregulated in the lungs of patients with IPF, and the expression of active TGF-β1 in the lungs of rats induces a dramatic fibrotic response, whereas an inability to respond to TGF-β1 affords protection from BLM-induced fibrosis [49]. The findings reported herein indicate that CO-HbV significantly reduced the active TGF-β1 content in lung tissue induced by the BLM treatment (Figure 7). Several *in vitro* studies showed that ROS and inflammatory cytokines promoted TGF-β1 production in pulmonary epithelial cells and its subsequent activation [50, 51]. Hence, these findings suggest that the suppression of ROS production and inflammatory cell infiltration at an early-stage of BLM treatment by CO-HbV eventually led to the suppression of active TGF-β1 production. In addition, it was reported that CO also suppressed TGF-β1-induced fibronectin and collagen

production by fibroblasts and that this process was dependent, in part, on the transcriptional regulator Id1 [52]. It thus appears that CO inhibits both TGF-β1 production and some of TGF-β1 mediated signal pathways in the lung, and subsequently decreases the deposition of fibronectin and collagen, resulting in the suppression of pulmonary fibrosis.

Since the benefit of CO as a therapeutic agent has already been revealed pre-clinically in animal models of various human diseases [8], CO-HbV may not only be an effective therapeutic agent for the treatment of IPF, but also against other diseases in which the Nox family of proteins play an important role in disease progression, such as heart disease, rheumatoid arthritis, sepsis and cancer [53]. However, for clinical application of CO-HbV, there are a number of concern, particularly in relation to HbV as a carrier. Fortunately, it has already been demonstrated that HbV can be used safely as a carrier in animals, that HbV possesses a high biocompatibility, a low toxicity and does not accumulate in the body [54, 55], indicating that HbV has the potential to function as a carrier of CO to diseased tissues in need of treatment without any detectable adverse effects. In addition, HbV has a good retention in the blood circulation in cynomolgus monkeys [23], and the half-life of HbV in humans was estimated to be approximately 3-4 days [56], which is long enough to function as a CO carrier. Furthermore, it is known that PEGylated liposmes show some unexpected pharmacokinetic properties, the so-called accelerated blood clearance phenomenon in which the long-circulation half-life is lost after being administered twice to the same animals [57]. Therefore, it is also concerned the pharmacokinetic properties after repeated infusion of CO-HbV, because it is expected that multiple injection of CO-HbV must be given for chronic and progressive diseases. In

previous study, we demonstrated that the pharmacokinetics of HbV were negligibly affected by repeated injections at a massive dose [55].

Conclusions

The findings reported herein demonstrate that CO-HbV can inhibit the progression of pulmonary fibrosis. Furthermore, it can also be concluded that CO-derived anti-inflammatory and anti-oxidant effects are involved in its suppressive effect against pulmonary fibrosis progression and loss of lung mechanics. CO-HbV could be a new type of pharmaceutical therapeutic agent for using CO as a medical gas that would arrest ROS and inflammation-related disorders.

Acknowledgement

This work was supported in part by Health Sciences Research Grants from the Ministry of Health, Labour and Welfare of Japan (201208035) and by a Grant-in-Aid for Young Scientist (B) from the Japan Society for the Promotion of Science (JSPS) (KAKENHI 24790159).

References

[1] Bjoraker JA, Ryu JH, Edwin MK, Myers JL, Tazelaar HD, Schroeder DR, et al. Prognostic significance of histopathologic subsets in idiopathic pulmonary fibrosis. Am J Respir Crit Care Med. 1998;157:199-203.

[2] King TE, Jr., Tooze JA, Schwarz MI, Brown KR, Cherniack RM. Predicting survival in idiopathic pulmonary fibrosis: scoring system and survival model. Am J Respir Crit Care Med. 2001;164:1171-81.

[3] Schwartz DA, Helmers RA, Galvin JR, Van Fossen DS, Frees KL, Dayton CS, et al. Determinants of survival in idiopathic pulmonary fibrosis. Am J Respir Crit Care Med. 1994;149:450-4.

[4] Noble PW, Albera C, Bradford WZ, Costabel U, Glassberg MK, Kardatzke D, et al. Pirfenidone in patients with idiopathic pulmonary fibrosis (CAPACITY): two randomised trials. Lancet. 2011;377:1760-9.

[5] Rafii R, Juarez MM, Albertson TE, Chan AL. A review of current and novel therapies for idiopathic pulmonary fibrosis. J Thorac Dis. 2013;5:48-73.

[6] Felton VM, Borok Z, Willis BC. N-acetylcysteine inhibits alveolar epithelial-mesenchymal transition. Am J Physiol Lung Cell Mol Physiol. 2009;297:L805-12.

[7] Gurrieri C, Piazza F, Gnoato M, Montini B, Biasutto L, Gattazzo C, et al. 3-(2,4-dichlorophenyl)-4-(1-methyl-1H-indol-3-yl)-1H-pyrrole-2,5-dione (SB216763), a glycogen synthase kinase-3 inhibitor, displays therapeutic properties in a mouse model of pulmonary inflammation and fibrosis. J Pharmacol Exp Ther. 2010;332:785-94.

[8] Motterlini R, Otterbein LE. The therapeutic potential of carbon monoxide. Nat Rev Drug Discov. 2010;9:728-43.

[9] Otterbein LE, Zuckerbraun BS, Haga M, Liu F, Song R, Usheva A, et al. Carbon monoxide suppresses arteriosclerotic lesions associated with chronic graft rejection and with balloon injury. Nat Med. 2003;9:183-90.

[10] Gentile MA. Inhaled medical gases: more to breathe than oxygen. Respir Care. 2011;56:1341-57; discussion 57-9.

[11] Motterlini R, Mann BE, Foresti R. Therapeutic applications of carbon monoxide-releasing molecules. Expert Opin Investig Drugs. 2005;14:1305-18.

[12] Chora AA, Fontoura P, Cunha A, Pais TF, Cardoso S, Ho PP, et al. Heme oxygenase-1 and carbon monoxide suppress autoimmune neuroinflammation. J Clin Invest. 2007;117:438-47.

[13] Ferrandiz ML, Maicas N, Garcia-Arnandis I, Terencio MC, Motterlini R, Devesa I, et al. Treatment with a CO-releasing molecule (CORM-3) reduces joint inflammation and erosion in murine collagen-induced arthritis. Ann Rheum Dis. 2008;67:1211-7.

[14] Hegazi RA, Rao KN, Mayle A, Sepulveda AR, Otterbein LE, Plevy SE. Carbon monoxide ameliorates chronic murine colitis through a heme oxygenase 1-dependent pathway. J Exp Med. 2005;202:1703-13.

[15] Ameredes BT, Otterbein LE, Kohut LK, Gligonic AL, Calhoun WJ, Choi AM. Low-dose carbon monoxide reduces airway hyperresponsiveness in mice. Am J Physiol Lung Cell Mol Physiol. 2003;285:L1270-6.

[16] Dubuis E, Potier M, Wang R, Vandier C. Continuous inhalation of carbon monoxide attenuates hypoxic pulmonary hypertension development presumably through activation of BKCa channels. Cardiovasc Res. 2005;65:751-61.

[17] Fujita T, Toda K, Karimova A, Yan SF, Naka Y, Yet SF, et al. Paradoxical rescue from ischemic lung injury by inhaled carbon monoxide driven by derepression of

fibrinolysis. Nat Med. 2001;7:598-604.

[18] Foresti R, Bani-Hani MG, Motterlini R. Use of carbon monoxide as a therapeutic agent: promises and challenges. Intensive Care Med. 2008;34:649-58.

[19] Omaye ST. Metabolic modulation of carbon monoxide toxicity. Toxicology. 2002;180:139-50.

[20] Abe H, Azuma H, Yamaguchi M, Fujihara M, Ikeda H, Sakai H, et al. Effects of hemoglobin vesicles, a liposomal artificial oxygen carrier, on hematological responses, complement and anaphylactic reactions in rats. Artif Cells Blood Substit Immobil Biotechnol. 2007;35:157-72.

[21] Sakai H, Suzuki Y, Sou K, Kano M. Cardiopulmonary hemodynamic responses to the small injection of hemoglobin vesicles (artificial oxygen carriers) in miniature pigs. J Biomed Mater Res A. 2012;100:2668-77.

[22] Sakai H, Masada Y, Horinouchi H, Ikeda E, Sou K, Takeoka S, et al. Physiological capacity of the reticuloendothelial system for the degradation of hemoglobin vesicles (artificial oxygen carriers) after massive intravenous doses by daily repeated infusions for 14 days. J Pharmacol Exp Ther. 2004;311:874-84.

[23] Taguchi K, Watanabe H, Sakai H, Horinouchi H, Kobayashi K, Maruyama T, et al. A fourteen-day observation and pharmacokinetic evaluation after a massive intravenous infusion of hemoglobin-vesicles (artificial oxygen carriers) in cynomolgus monkeys. J Drug Metab Toxicol. 2012;3:128.

[24] Sakai H, Horinouchi H, Masada Y, Takeoka S, Ikeda E, Takaori M, et al. Metabolism of hemoglobin-vesicles (artificial oxygen carriers) and their influence on organ functions in a rat model. Biomaterials. 2004;25:4317-25.

[25] Sakai H, Horinouchi H, Tsuchida E, Kobayashi K. Hemoglobin vesicles and red

blood cells as carriers of carbon monoxide prior to oxygen for resuscitation after hemorrhagic shock in a rat model. Shock. 2009;31:507-14.

[26] Sakai H, Takeoka S, Park SI, Kose T, Nishide H, Izumi Y, et al. Surface modification of hemoglobin vesicles with poly(ethylene glycol) and effects on aggregation, viscosity, and blood flow during 90% exchange transfusion in anesthetized rats. Bioconjug Chem. 1997;8:23-30.

[27] Tanaka R, Watanabe H, Kodama A, Chuang VT, Ishima Y, Hamasaki K, et al. Long-acting human serum albumin-thioredoxin fusion protein suppresses bleomycin-induced pulmonary fibrosis progression. J Pharmacol Exp Ther. 2013;345:271-83.

[28] Sakai H, Tomiyama K, Masada Y, Takeoka S, Horinouchi H, Kobayashi K, et al. Pretreatment of serum containing hemoglobin vesicles (oxygen carriers) to prevent their interference in laboratory tests. Clin Chem Lab Med. 2003;41:222-31.

[29] Furukawa M, Tanaka R, Chuang VT, Ishima Y, Taguchi K, Watanabe H, et al. Human serum albumin-thioredoxin fusion protein with long blood retention property is effective in suppressing lung injury. J Control Release. 2011;154:189-95.

[30] Woessner JF, Jr. The determination of hydroxyproline in tissue and protein samples containing small proportions of this imino acid. Arch Biochem Biophys. 1961;93:440-7.

[31] Tanaka K, Azuma A, Miyazaki Y, Sato K, Mizushima T. Effects of lecithinized superoxide dismutase and/or pirfenidone against bleomycin-induced pulmonary fibrosis. Chest. 2012;142:1011-9.

[32] Kim-Mitsuyama S, Yamamoto E, Tanaka T, Zhan Y, Izumi Y, Izumiya Y, et al. Critical role of angiotensin II in excess salt-induced brain oxidative stress of stroke-prone spontaneously hypertensive rats. Stroke. 2005;36:1083-8.

[33] Keane MP, Strieter RM. The importance of balanced pro-inflammatory and anti-inflammatory mechanisms in diffuse lung disease. Respir Res. 2002;3:5.

[34] Piguet PF, Ribaux C, Karpuz V, Grau GE, Kapanci Y. Expression and localization of tumor necrosis factor-alpha and its mRNA in idiopathic pulmonary fibrosis. Am J Pathol. 1993;143:651-5.

[35] Hunninghake GW. Antioxidant therapy for idiopathic pulmonary fibrosis. N Engl J Med. 2005;353:2285-7.

[36] Amara N, Goven D, Prost F, Muloway R, Crestani B, Boczkowski J. NOX4/NADPH oxidase expression is increased in pulmonary fibroblasts from patients with idiopathic pulmonary fibrosis and mediates TGFbeta1-induced fibroblast differentiation into myofibroblasts. Thorax. 2010;65:733-8.

[37] Hecker L, Vittal R, Jones T, Jagirdar R, Luckhardt TR, Horowitz JC, et al. NADPH oxidase-4 mediates myofibroblast activation and fibrogenic responses to lung injury. Nat Med. 2009;15:1077-81.

[38] Lyle AN, Deshpande NN, Taniyama Y, Seidel-Rogol B, Pounkova L, Du P, et al. Poldip2, a novel regulator of Nox4 and cytoskeletal integrity in vascular smooth muscle cells. Circ Res. 2009;105:249-59.

[39] Mauviel A. Transforming growth factor-beta: a key mediator of fibrosis. Methods Mol Med. 2005;117:69-80.

[40] Raghu G, Collard HR, Egan JJ, Martinez FJ, Behr J, Brown KK, et al. An official ATS/ERS/JRS/ALAT statement: idiopathic pulmonary fibrosis: evidence-based guidelines for diagnosis and management. Am J Respir Crit Care Med. 2011;183:788-824.

[41] Taguchi K, Urata Y, Anraku M, Maruyama T, Watanabe H, Sakai H, et al.

Pharmacokinetic study of enclosed hemoglobin and outer lipid component after the administration of hemoglobin vesicles as an artificial oxygen carrier. Drug Metab Dispos. 2009;37:1456-63.

[42] Cantin AM, North SL, Fells GA, Hubbard RC, Crystal RG. Oxidant-mediated epithelial cell injury in idiopathic pulmonary fibrosis. J Clin Invest. 1987;79:1665-73.

[43] Strausz J, Muller-Quernheim J, Steppling H, Ferlinz R. Oxygen radical production by alveolar inflammatory cells in idiopathic pulmonary fibrosis. Am Rev Respir Dis. 1990;141:124-8.

[44] Manoury B, Nenan S, Leclerc O, Guenon I, Boichot E, Planquois JM, et al. The absence of reactive oxygen species production protects mice against bleomycin-induced pulmonary fibrosis. Respir Res. 2005;6:11.

[45] Nakahira K, Kim HP, Geng XH, Nakao A, Wang X, Murase N, et al. Carbon monoxide differentially inhibits TLR signaling pathways by regulating ROS-induced trafficking of TLRs to lipid rafts. J Exp Med. 2006;203:2377-89.

[46] Carnesecchi S, Deffert C, Donati Y, Basset O, Hinz B, Preynat-Seauve O, et al. A key role for NOX4 in epithelial cell death during development of lung fibrosis. Antioxid Redox Signal. 2011;15:607-19.

[47] Serrander L, Cartier L, Bedard K, Banfi B, Lardy B, Plastre O, et al. NOX4 activity is determined by mRNA levels and reveals a unique pattern of ROS generation. Biochem J. 2007;406:105-14.

[48] Willis BC, Borok Z. TGF-beta-induced EMT: mechanisms and implications for fibrotic lung disease. Am J Physiol Lung Cell Mol Physiol. 2007;293:L525-34.

[49] Zhao J, Shi W, Wang YL, Chen H, Bringas P, Jr., Datto MB, et al. Smad3 deficiency attenuates bleomycin-induced pulmonary fibrosis in mice. Am J Physiol Lung Cell Mol

Physiol. 2002;282:L585-93.

[50] Barcellos-Hoff MH, Dix TA. Redox-mediated activation of latent transforming growth factor-beta 1. Mol Endocrinol. 1996;10:1077-83.

[51] Bellocq A, Azoulay E, Marullo S, Flahault A, Fouqueray B, Philippe C, et al. Reactive oxygen and nitrogen intermediates increase transforming growth factor-beta1 release from human epithelial alveolar cells through two different mechanisms. Am J Respir Cell Mol Biol. 1999;21:128-36.

[52] Zhou Z, Song R, Fattman CL, Greenhill S, Alber S, Oury TD, et al. Carbon monoxide suppresses bleomycin-induced lung fibrosis. Am J Pathol. 2005;166:27-37.

[53] Al Ghouleh I, Khoo NK, Knaus UG, Griendling KK, Touyz RM, Thannickal VJ, et al. Oxidases and peroxidases in cardiovascular and lung disease: new concepts in oxygen species signaling. Free Radic Biol Med. 2011;51:1271-88.

[54] Sakai H. Present situation of the development of cellular-type hemoglobin-based oxygen carrier (hemoglobin-vesicles). Curr Drug Discov Technol. 2012;9:188-93.

[55] Taguchi K, Maruyama T, Otagiri M. Pharmacokinetic properties of hemoglobin vesicles as a substitute for red blood cells. Drug Metab Rev. 2011;43:362-73.

[56] Taguchi K, Maruyama T, Iwao Y, Sakai H, Kobayashi K, Horinouchi H, et al. Pharmacokinetics of single and repeated injection of hemoglobin-vesicles in hemorrhagic shock rat model. J Control Release. 2009; 136:232-9.

[57] Abu Lila AS, Kiwada H, Ishida T. The accelerated blood clearance (ABC) phenomenon: clinical challenge and approaches to manage. J Control Release. 2013; 172:38-47.

Captions

Click here to download Captions: caption.docx

Figure legends

Figure 1

Structures of hemoglobin-vesicles and its lipid components.

Figure 2

CO-HbV affects BLM-induced pulmonary fibrosis in a dose-dependent manner. (A) *Outline of the experimental design.* Mice were treated with bleomycin (BLM, 5 mg/kg) once on day 0. They were also administered by CO-HbV *via* the tail vein at 30 min before BLM treatment and 24 hour after BLM treatment. (B) *Histopathologic evaluation at after CO-HbV treatment on day 14 in BLM-induced pulmonary fibrosis mice.* Sections of pulmonary tissues were prepared on day 14 and subjected to hematoxylin and eosin staining (upper panels) and Masson trichrome staining (lower panels). (C) *Hydroxyproline leveles in left lung at after CO-HbV treatment on day 14 in BLM-induced pulmonary fibrosis mice.* The pulmonary hydroxyproline level was determined on day 14 as described in the "Materials and Methods" section. Each value represents the mean ± s.d. (n=5-6). **P<0.01 versus control. †P<0.05 versus CO-HbV.

Figure 3

Effects of CO-HbV against bleomycin-induced pulmonary fibrosis and alterations in lung mechanics.

(A) *The weight differences during 14 days after BLM treatment.* Mice were treated with bleomycin (BLM, 5 mg/kg) once on day 0. They were also administered with saline, HbV (1000 mg Hb/kg) or CO-HbV (1000 mg Hb/kg) *via* the tail vein at 30 min before BLM treatment and 24 hour after BLM treatment. Each value represents the mean ± s.d. (n=4-5). (B) *Histopathologic evaluation at after saline, HbV or CO-HbV treatment on day 14 in BLM-induced pulmonary fibrosis mice.* Sections of pulmonary tissue were prepared on day 14 and subjected to hematoxylin and eosin staining (upper panels) and Masson trichrome staining (lower panels). (C) *Hydroxyproline leveles in left lung at after saline, HbV or CO-HbV treatment on day 14 in BLM-induced pulmonary fibrosis mice.* The pulmonary hydroxyproline level was done on day 14 as described in Figure 2 legend. Each value represents the mean ± s.d. (n=3-7). **P<0.01 versus control. ††P<0.01 versus CO-HbV. (D-F) *The lung mechanics and respiratory functions at after saline, HbV or CO-HbV treatment on day 14 in BLM-induced pulmonary fibrosis mice.* Forced vital capacity (D), total respiratory system elastance (E) and tissue elastance (F) were determined on day 14 as described in the "Materials and Methods" section. Each value represents the mean ± s.d. (n=4-5). **P<0.01 versus control. ††P<0.01 versus CO-HbV. †P<0.05 versus CO-HbV.

Figure 4

Effect of CO-HbV on cells in bronchoalveolar lavage fluid in bleomycin-induced pulmonary fibrosis mice.

The number of inflammatory cells including (a) total cells, (b) alveolar macrophages and (c) neutrophils in bronchoalveolar lavage fluid on day 3. These inflammatory cells were determined on day 3 as described in the "Materials and Methods" section. Each value represents the mean ± s.d. (n=3-6). **P<0.01 versus control. ††P<0.01 versus CO-HbV. †P<0.05 versus CO-HbV.

Figure 5

Effect of CO-HbV on pulmonary inflammatory cytokines and chemokines in bleomycin-induced pulmonary fibrosis mice.

The levels of cytokines and chemokine including (a) TNF-α, (b) IL-6 and (c) IL-1β in lung tissue on day 7. The amount of inflammatory cytokines and chemokine in whole lung tissue was measured by ELISA kit as described in the "Materials and Methods" section. Each value represents the mean ± s.d. (n=5). **P<0.01 versus control. ††P<0.01 versus CO-HbV. †P<0.05 versus CO-HbV.

Figure 6

Effect of CO-HbV on the generation of reactive oxygen species in lung tissue in bleomycin-induced pulmonary fibrosis mice.

(A) *The immunostaining of the lungs slice for the oxidative stress markers of nucleic acid (8-OH-dG; upper) and amino acid (NO_2-Tyr; lower).* Mice were treated with bleomycin (BLM, 5 mg/kg) once on day 0. They were also administered saline, HbV or CO-HbV *via* the tail vein at 30 min before BLM treatment and 24 hour after BLM treatment. Subsequently, the each immunostaining was performed on day 3 after BLM administration. (B) *Production of pulmonary superoxide in bleomycin-induced pulmonary fibrosis mice on day 7 after BLM administration.* Dihydroethidium was used to evaluate lung superoxide concentrations. *(C-D)The protein expression of nicotinamide adenine dinucleotide phosphate oxidase 4 (Nox4) in lung tissue.* Protein expression levels of Nox4 was determined by (C) immunostaining and (D) western blotting as described in the "Materials and Methods" section. *The protein expression of (E) $p22^{phox}$ and (F) polymerase delta interacting protein 2 (Poldip2)in lung tissue.* Protein expression levels of both $p22^{phox}$ and Poldip2 were determined by western blotting as described in the "Materials and Methods" section.

Figure 7

Effect of CO-HbV on active TGF-β1 levels in bleomycin-induced pulmonary fibrosis mice.

Active TGF-β1 levels in lung were determined on day 7 as described in the "Materials and Methods" Each value represents the mean ± s.d. (n=6). ††P<0.01 versus CO-HbV.

Table
Click here to download Table: Table.docx

Table 1

Plasma clinical chemistry test results in control mice and BLM-induced pulmonary fibrosis mice after saline, HbV and CO-HbV administration.

		Day 7			Day 14		
	control	BLM+saline	BLM+HbV	BLM+CO-HbV	BLM+saline	BLM+HbV	BLM+CO-HbV
AST	34.8±3.5	67.3±18.5	73.7±20.3	74.0±24.3	61.7±35.0	53.8±7.3	52.9±16.8
ALT	23.9±3.6	46.3±14.7	62.0±17.3	61.0±28.6	43.1±21.0	33.0±7.9	37.0±15.1
ALP	317.9±66.2	315.7±106.4	302.8±67.3	334.0±75.8	313.8±39.2	357.8±54.0	324.3±65.1
BUN	22.7±3.7	28.3±3.3	27.8±5.0	30.0±5.4	22.2±3.3	24.1±3.1	22.6±1.8
CRE	0.10±0.03	0.14±0.02	0.10±0.03	0.13±0.03	0.10±0.02	0.11±0.01	0.10±0.01
CK	105.6±35.7	130.3±55.6	105.2±48.3	96.5±29.9	224.9±255.8	69.4±22.1	70.3±15.2
LDH	152.6±42.1	301.4±135.2	341.0±63.6	258.7±66.1	263.0±141.5	278.2±90.5	237.4±45.0
AMY	2052.1±318.2	2739.7±459.7	2619.7±457.1	2480.3±347.4	2036.9±335.1	2520.0±394.6	2292.4±295.7
T-CHO	125.6±24.1	119.1±25.9	160.7±25.1	143.0±23.8	127.7±13.9	118.4±16.4	131.3±23.9

AST, aspartate aminotransferase; ALT, alanine aminotransferase; ALP, alkaline phosphatase; BUN, urea nitrogen; CRE, creatinine; CK, creatine kinase; LDH, lactate dehydrogenase; AMY, amylase; T-CHO, total cholesterol

Figure
Figure 1
Click here to download Figure: Figure_1.pdf

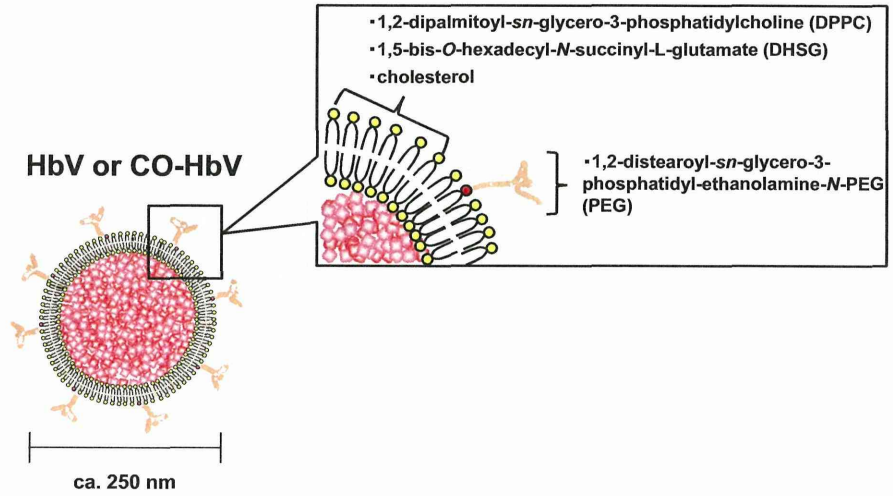

Figure
Figure 2

Click here to download Figure: Figure_2.pdf

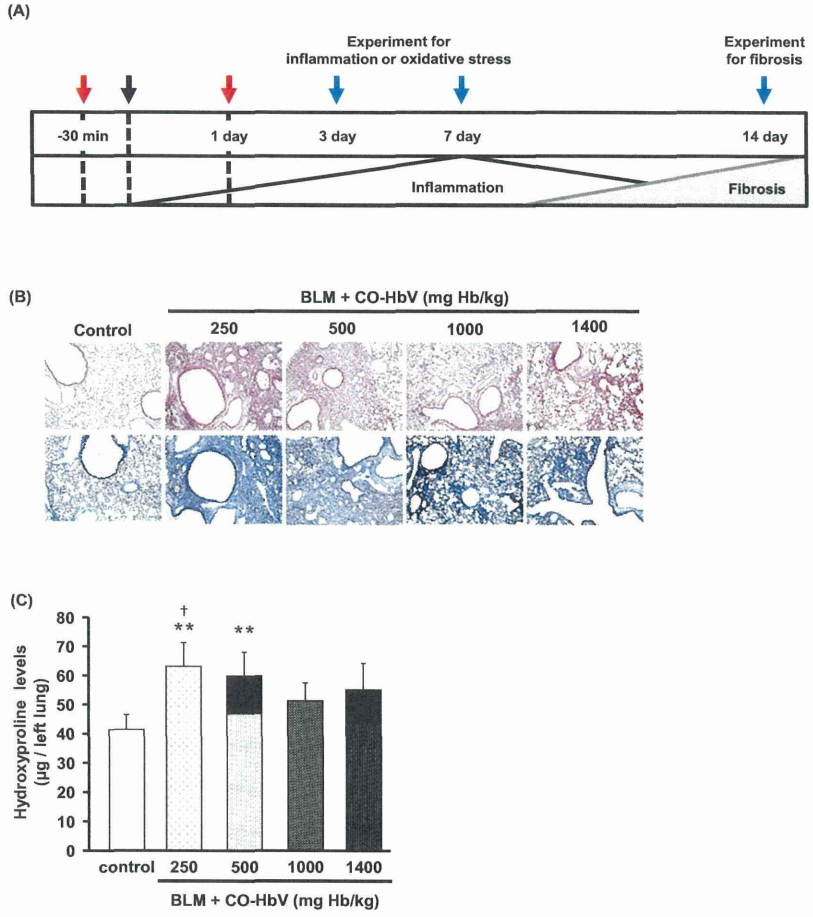

Figure
Figure 3

Click here to download Figure: Figure_3.pdf

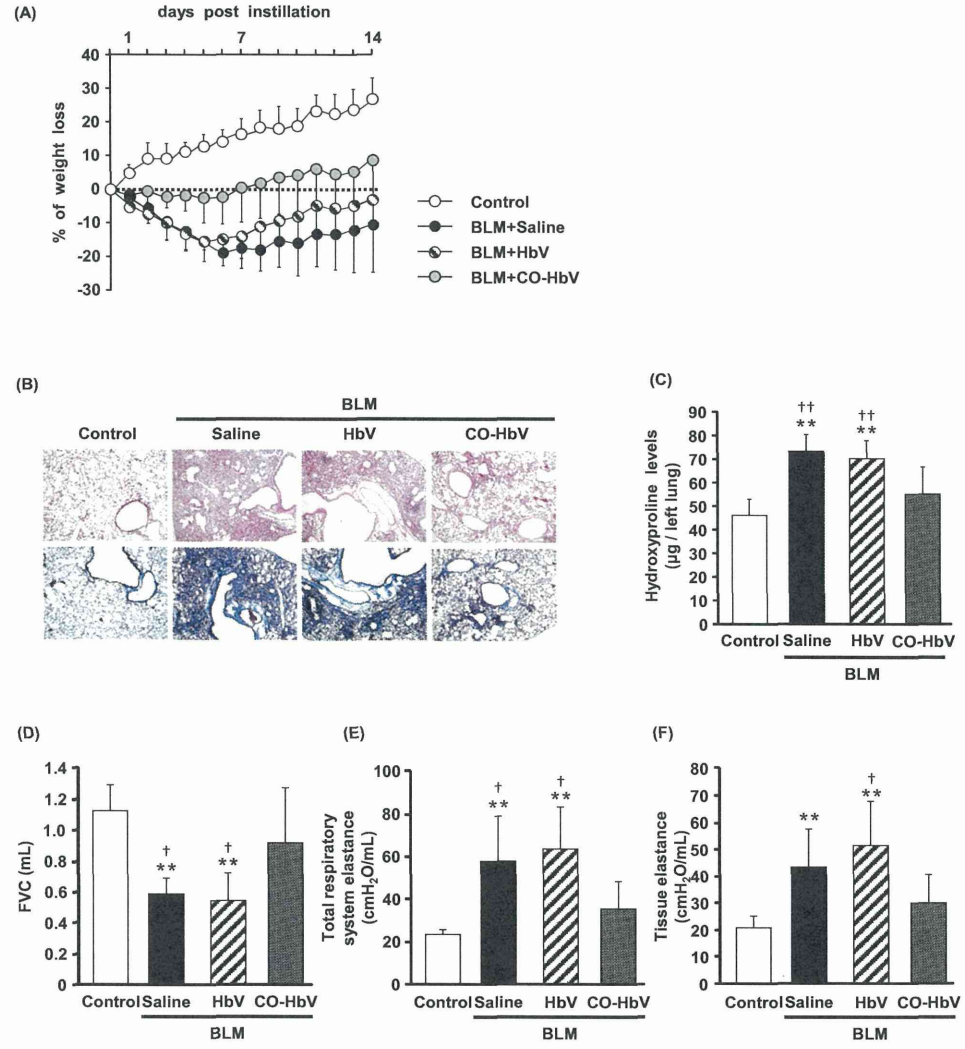

Figure 4

Click here to download Figure: Figure_4.pdf

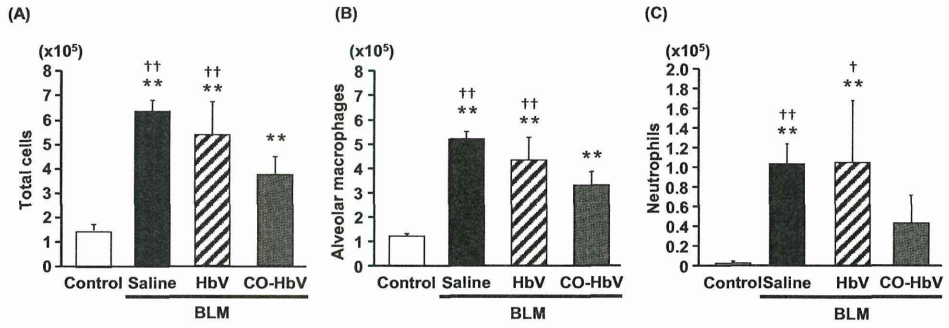

Figure 5

Click here to download Figure: Figure_5.pdf

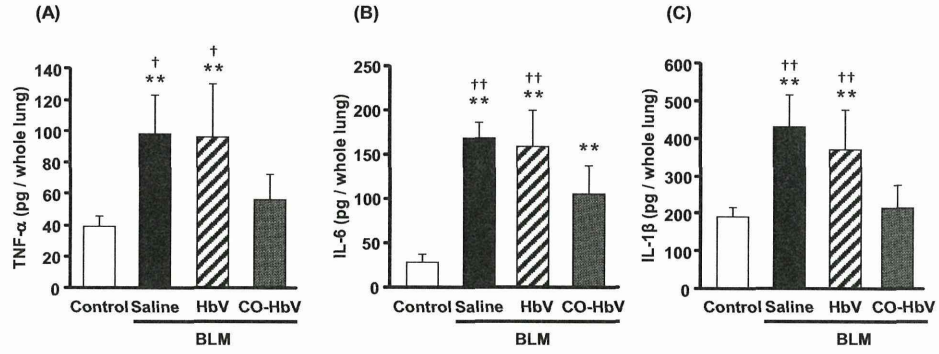

Figure
Figure 6
Click here to download Figure: Figure_6.pdf

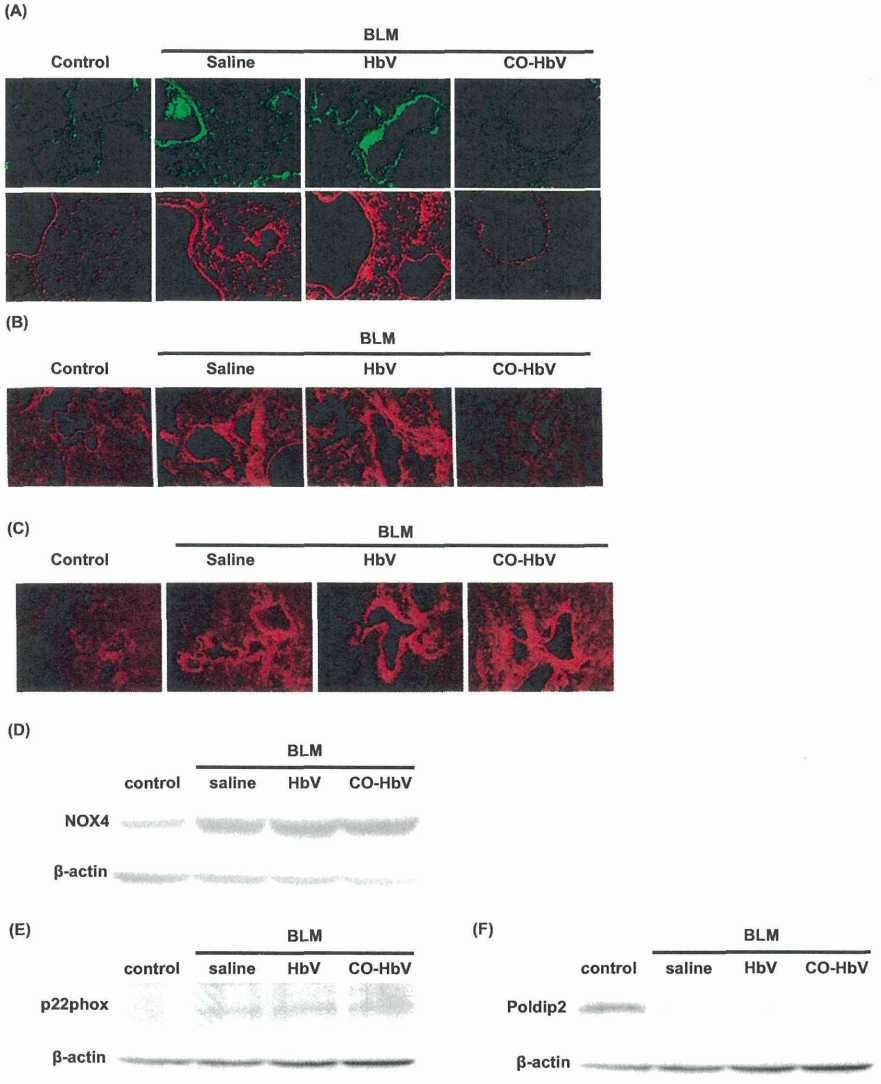

Figure
Figure 7
Click here to download Figure: Figure_7.pdf

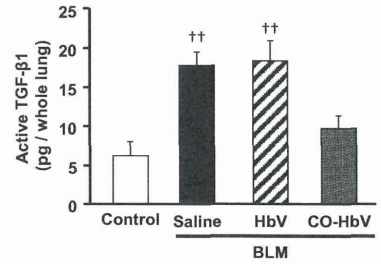

● 一般演題

出血性ショック心臓における致死性不整脈の機序に関する実験的検討

—活動電位不均一性とConnexin43変化について—

防衛医科大学校集中治療部　髙瀬凡平・東村悠子・木村一生
防衛医学研究センター医療工学研究部門　田中良弘・服部秀美・石原雅之

要　約

出血性ショックにより平均全身血圧が40mmHg以下に低下遷延すると，不可逆性心筋障害が発生し，いわゆる“出血性ショック心臓”といわれる致死性の病態を呈するとされている。しかし，致死性不整脈の発生機序に関する検討は少ない。そこでわれわれは，実験的に検討した。

方法：SD rat（$n=32$）に30%出血性ショック状態を作製し，非蘇生群，洗浄赤血球蘇生群，生理食塩水蘇生群，5%アルブミン蘇生群の4群間で心筋を摘出Tyrode液で灌流後Na channel感受性色素を用いたoptical mapping system（OMP）で興奮伝播・活動電位持続時間不均一性（action potential duration dispersion：APD dispersion），致死性催不整脈性を検討した。また，心筋組織のconnexin43（Cx43）発現を免疫組織染色にて検討した。

結果：蘇生群では，3群とも全例蘇生に成功した。しかし，生理食塩水群，5%アルブミン群ではOMPで著明な左心室伝導遅延とburst pacingによる心室細動が全例で誘発されたのに対し，洗浄赤血球蘇生群では，伝導遅延・心室細動誘発ともに認められなかった。生理食塩水群，5%アルブミン群では著明にAPD dispersion値が増大したが，洗浄赤血球群では正常に保たれていた。connexin43発現は生理食塩水群，5%アルブミン群では異常が認められたものの，洗浄赤血球群では正常に保たれていた。

結語：出血性ショック心臓では，左心室伝導遅延とAPD dispersion増大およびconnexin43発現異常を惹起し，電気的不安定性から致死性不整脈が誘発されることが示唆された。洗浄赤血球治療はこれら指標の保持と予防効果を有した。

はじめに

これまでの多くの研究や臨床診療において心筋機能障害や心不全は遷延する出血性ショックに伴って頻繁に認められるとされている[1,2]。これらは，出血性ショックからの一時的回復後の予後不良および出血性ショック時の致死的血行動態破綻にかかわる。先行研究によると，出血性ショックに伴う心筋虚血や心筋低酸素状態が出血性ショック時の致死性心筋機能障害を惹起すると報告されている[3]。出血性ショックの心臓への致命的障害を回避するためには，出血性ショックからの迅速な回復や心筋への重篤な虚血や低酸素血症を未然に防ぐ有効な治療が必要である[4]。

また，出血性ショック・蘇生は，心筋全体の虚血・再還流である。さらに，平均全身血圧が

Bonpei Takase, et al. : Significant role of action potential duration dispersion and connexin 43 in lethal arrhythmogenesis in hemorrhagic shock heart: optical mapping analysis

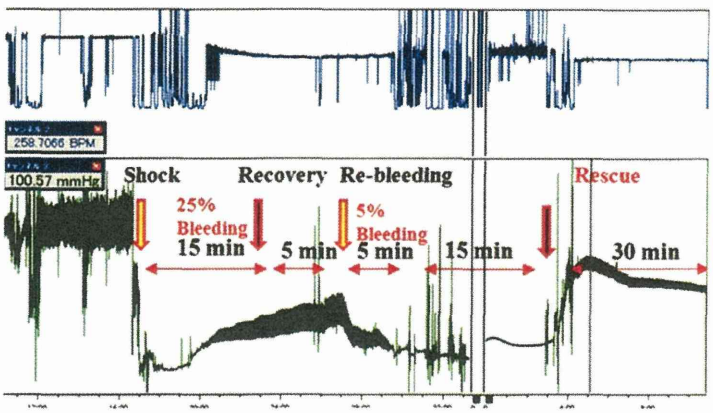

図1　出血性ショックモデルの作製プロトコール

40mmHg以下に低下遷延すると，不可逆性心筋障害が発生し，いわゆる"出血性ショック心臓"といわれる致死性の病態を呈するとも報告されている[5]。しかし，"出血性ショック心臓"の蘇生後の致死性不整脈出現やその病態に関する検討は少ない。

そこで，実験的に30%出血性ショック状態を作製し，5%アルブミン，生理食塩水，洗浄赤血球で蘇生した3群で心筋を摘出しTyrode液で灌流後Na^+ channel 感受性色素を用いたoptical mapping systemで興奮伝播・活動電位持続時間不均一性(APD dispersion)および致死性催不整脈誘発性を検討するとともに，心筋組織の心筋興奮伝導蛋白であるconnexin43発現[6]を免疫組織染色し，非蘇生群を対照群として，出血性ショック心の不整脈発生機序を検討することを本研究の目的とした。

1　方　　法

Sprague-Dawley rats (male；8 weeks old；250～300 g；$n=32$)の皮下にketamine hydrochloride (5mg/kg)を投与し麻酔した。麻酔下に気管内挿管し，人工呼吸下でabdominal aorta catheterを挿入して，血圧測定するとともにabdominal aorta catheterから脱血し，以下のプロトコールで致死性出血性ショックモデルを作製した(**図1**)。すなわち，循環血液量25%を15分で脱血，5分間放置後再出血モデルとして，5%を5分かけて再脱血(Total 30% blood loss：不可逆性ショック)を実施した。その後15分間放置したのち，脱血量と同量で①5%アルブミン(5%アルブミン群)，②生理食塩水(生理食塩水群)および③洗浄赤血球(洗浄赤血球群)蘇生した。また，④非蘇生群も対照群として作製した(各群，$n=8$)。

1) optical mapping analysis 法と不整脈誘発法

ラットを麻酔後，正中切開にて開胸し，迅速に心臓を摘出した。大動脈から冠動脈洞にカニューレを挿入した。酸素化し37℃に保温したTyrode 液($CaCl_2$ [2], NaCl [140], KCl [4.5], dextrose [10], $MgCl_2$ [1], and HEPES [10, pH 7.4] , in mmol/L)にてただちに灌流した。さらに，Tyrode液を一定容量で灌流している水槽に心臓を固定し，大動脈に挿入したカニューレからNa感受性蛍光色素(di-4-ANEPPS 15 μmol/L)を約40mL，2分間かけて灌流染色した。さらに，心臓の拍動を停止させるため2.3-butanedione monoxime (Wako Chemical, Tokyo, Japan, 20 mM) を灌流した。optical mapping analysisはhigh-quality charge couple

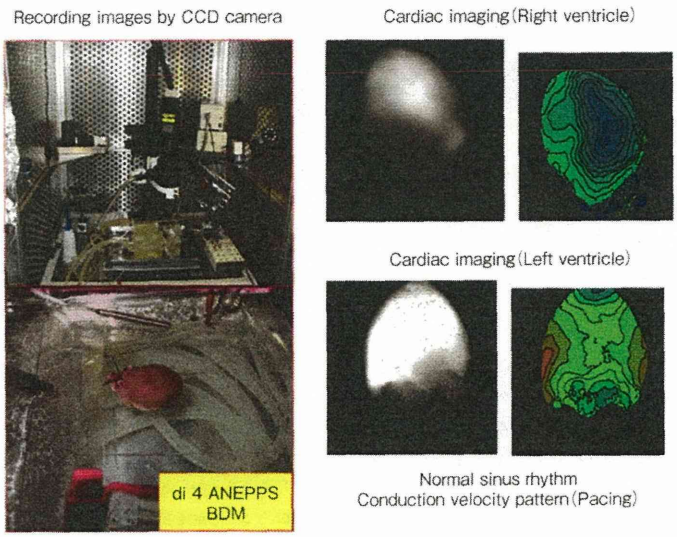

図2　optical mapping system と洞調律における左心室および右心室の正常な興奮伝播速度と伝播様式

device（CCD）camera（Leica 10447050, Geneva, Switzerland）を用いて4秒間撮像した。撮像は心筋が洞調律であることを確認してから，左心室，右心室外膜面の興奮伝播時間(ms)と伝播様式，得られた活動電位持続時間(APD)をcommercialized software（Ultima−6006；Sei Media, Inc., Tokyo, Japan)にて解析した(**図2**)。右心室心膜面の約5×5mmの関心部位(ほぼ右心室自由壁の中央)を任意に設定し，この部位におけるAPDの分布のヒストグラムと，APDの実波形を記録した。APDはAPD 60msを使用した。ヒストグラムより，最大APDと最小APDの差からAPD dispersion（ms)を決定し，出血性ショック蘇生後摘出心臓における，経時的APD dispersionの変化を比較した(**図3**)。

さらに，催不整脈性を調べるために，右心室・左心室の3ヵ所，すなわち右心室心尖部，心臓基部，右室流出路を20回の連続刺激(burst pacing, 5, 50, 100 V；40ms interval, 20 trains）各voltageにて3回ずつ施行し，致死性不整脈の誘発の有無を検討した(**図4A**)。

2）connexin43に関する免疫組織学的検討

摘出心臓を4% paraformaldehyde phosphate buffer solution（Wako Pure Chemical Industries Ltd.）にて48時間固定した。それぞれの標本は，70% ethanolにて脱水しparaffin固定した。組織学的検討では，心筋伝導蛋白であるconnexin43の心筋組織内発現の程度を定性的に評価するため，免疫組織染色を施行した。すなわち，anti−connexin43 monoclonal antibody（1：2,000, Sigma−Aldrich, St. Louis, USA）を用いて，心筋組織内の心筋 gap−junction蛋白connexin43の発現を検討した。

3）統計学的検討

各群において，興奮伝播時間およびAPD dispersionは平均±標準偏差で表した。興奮伝播様式およびconnexin43の発現様式は，異常あり，または，なしの定性的2分類でその頻度を検討し，致死性不整脈誘発頻度に関しても誘発の有無につき各個体ごとに検討し，その頻度を比較した。群間の比較にはANOVA法にて検定し，Bonferroni post hoc補正を実施した。頻度

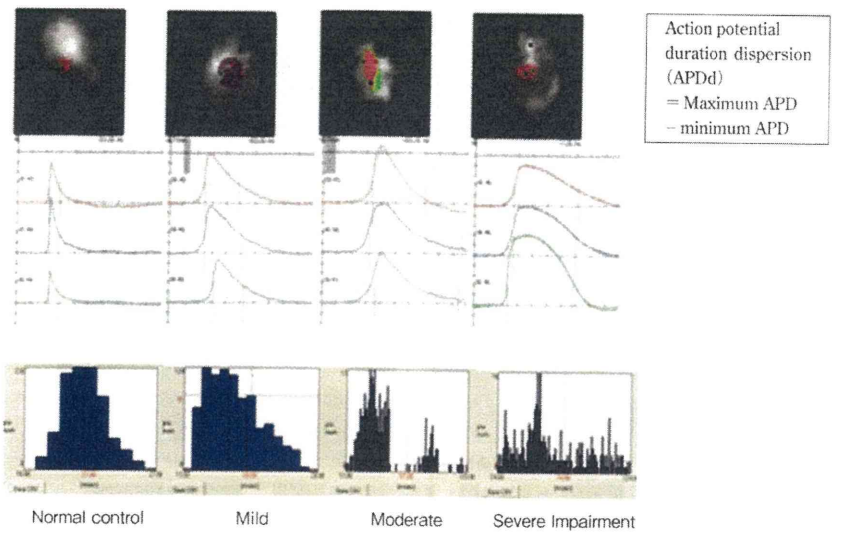

図3　optical mapping system における action potential duration dispersion 計測法と正常例および異常例の所見

の検定には χ^2 検定を実施した。$p<0.05$ を推計学的に有意とした。

2　結　　果

1）optical mapping analysis 法による興奮伝播時間・伝播様式および APD dispersion と不整脈誘発の結果

非蘇生群では全例ラットは心室細動または徐脈性不整脈を惹起し，その後心停止をきたした（**図4B**）。他の3群では，各蘇生液により全ラットの血行動態はショック状態から蘇生された。これら3群のラットから摘出された心臓の興奮伝播時間・伝播様式を optical mapping system にて検討した結果を**図5**に示した。

正常ラットの洞調律における左心室の興奮伝播時間は24±1msであり，伝播様式は**図2**に示したパターンであった。一方，5%アルブミン群および生理食塩水群では，ショック状態から蘇生されたにもかかわらず，興奮伝播時間はそれぞれ35±3msおよび39±3msと有意かつ著明に延長しており，伝播様式の明らかに正常パ

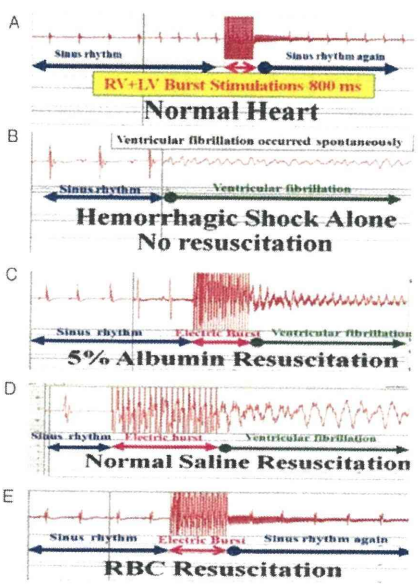

図4　非蘇生群，各蘇生群における左心室への burst pacing による致死性不整脈誘発による致死性不整脈発現様式

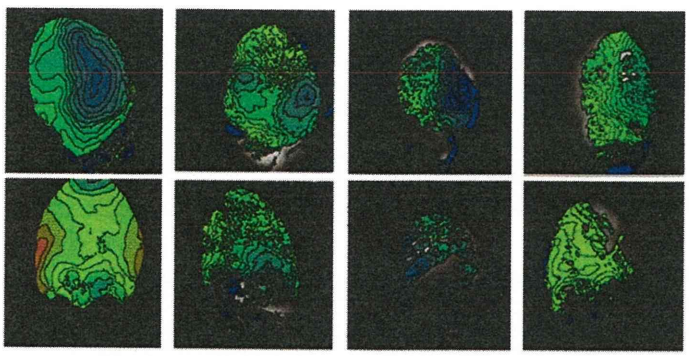

図5　心筋興奮伝播時間と伝播様式の比較

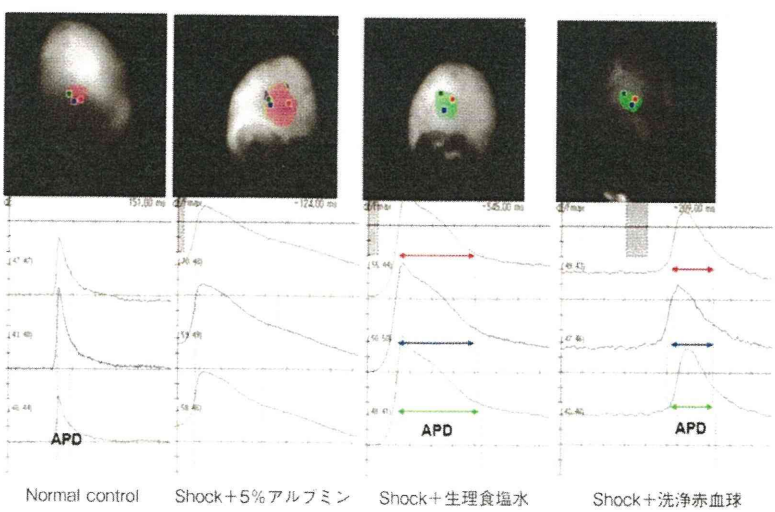

図6　action potential duration dispersionの比較

ターンと異なっていた(**図5**)。しかし，洗浄赤血球群で蘇生したラットでは，全例が正常興奮伝播時間(22±3ms)であり，かつ，正常伝播様式であることが認められた。さらにAPD dispersionは，洗浄赤血球群で全ラットが，**図3**で示したnormal controlと差を認めなかったのに対し(normal control vs 洗浄赤血球群：14±2ms vs 13±3ms, NS)，5％アルブミン群および生理食塩水群では全ラットで，**図3**で示したmoderateまたはsevere impairment patternを示し，APD dispersionはそれぞれ34±27msおよび38±9msと有意($p<0.05$)かつ著明に延長していた。また，APDそのものも正常ラット，洗浄赤血球群に比較し，5％アルブミン群および生